Journal of Catalysis **183,** 323–335 (1999)
Article ID jcat.1999.2414, available online at http://www.idealibrary.com on IDEAL®

Selective Catalytic Reduction of Nitric Oxide by Methane in the Presence of Oxygen over CaO Catalyst

K. D. Fliatoura,* X. E. Verykios,* C. N. Costa,† and A. M. Efstathiou†,[1]

*Department of Chemical Engineering, University of Patras, GR-26500 Patras, Greece; and †Department of Natural Sciences, University of Cyprus, P.O. Box 537, Nicosia, Cyprus

Received September 16, 1998; revised January 6, 1999; accepted January 6, 1999

The selective catalytic reduction of nitric oxide by methane in the presence of oxygen was studied over CaO catalyst in the temperature range 550–850°C. The nitric oxide conversion-versus-temperature profile was found to depend on oxygen feed concentration, while the selectivity to N_2 formation was found to be 100% and independent of oxygen feed concentration in the range 1–10 mol%. The kinetic study has shown that the reaction order with respect to NO and CH_4 is 1.0 and 0.5, respectively. On the other hand, the reaction order with respect to O_2 was found to be slightly positive for O_2 feed concentrations up to 1 mol% and slightly negative at higher concentrations. The apparent activation energy of the reaction in the presence of oxygen was found to be 14.6 kcal/mol. The addition of 2.5 mol% CO_2 and 5 mol% H_2O in the feed stream had a considerable inhibiting effect on NO conversion in the range 550–650°C, while a small inhibiting effect of CO_2 and a positive effect of H_2O were observed in the range 700–850°C. Temperature-programmed desorption (TPD) of NO revealed the presence of two well-resolved NO peaks in the temperature range 250–650°C, a behavior also observed during a temperature-programmed oxidation experiment under O_2/He flow. However, during temperature-programmed surface reaction under CH_4/He flow the NO desorption spectrum showed a significant shift of the stronger adsorbed NO species toward lower temperatures. Preadsorbed CO_2 on the CaO surface was found to largely affect the chemisorption of NO and its desorption kinetics during TPD. The amount of deposited carbon-containing species on the catalyst surface during reaction was determined with transient titration experiments and it was found to be small.

Key Words: **nitric oxide reduction by CH_4; NO reduction by hydrocarbon; nitrogen oxides; methane; calcium oxide; nitric oxide reduction kinetics.**

1. INTRODUCTION

Many processes have been developed in recent years for the removal of nitrogen oxides in flue gases from stationary and mobile sources. Selective catalytic reduction of NO_x with ammonia is among the most effective methods for controlling this hazardous emission from power stations (1, 2), but the use of NH_3 as a reducing agent poses problems of storage, transportation, high cost, and equipment corrosion. Recently, the selective catalytic reduction of nitric oxide with hydrocarbons (HC-SCR) has received increased attention from both academic and industrial points of view, because this may offer an effective way of removing NO even in the presence of a large excess of O_2 (3). Nitric oxide reduction using CH_4 as a reducing agent was studied as early as 1984 over Rh/Al_2O_3 catalysts (4). A variety of ion-exchanged zeolites, including Cu-, Fe-, Pt-, Co-, Ga-, Ce-, and H-exchanged zeolites have been found to be active for this reaction (5–11) but their suitability is limited due to a volcano-like activity dependence on temperature and their deactivation in the presence of large amounts of water. Currently, ethylene, propane, propylene, and *n*-octane hydrocarbons have been investigated for lean-NO_x reduction (12–16). Methane is regarded as a nonselective reducing agent because it is difficult to activate due to the very strong C–H bond which necessitates high reaction temperatures (10, 17, 18). On the other hand, with the abundance of natural gas and its widespread use as a fuel by many utilities, it certainly would be desirable to use methane as a reducing agent. Thus, the investigation of new catalytic systems that can effectively reduce NO with CH_4 at relatively high temperatures has attracted attention (19–23).

The reactivity of $CH_3\cdot$ radicals with NO and NO_2 is well established in homogeneous gas-phase reactions (24–27). Vannice and co-workers hypothesized that an increase in methyl radical concentration would enhance the overall reaction between CH_4 and NO and they chose several methane oxidative coupling catalytic systems to investigate. They found that MgO, Li/MgO, and several rare earth oxide catalysts are active for either decomposition of NO or its reduction by methane in both the absence and presence of oxygen (19–23). However, the true reaction pathways of NO reduction with CH_4 in the presence of oxygen over metal oxide catalytic surfaces remain an open question to investigate.

Campbell *et al.* (28) have indicated that the activities of oxidative coupling of methane (OCM) metal oxides for the

[1] To whom correspondence should be addressed. Fax: (3572) 339060. E-mail: efstath@ucy.ac.cy.

0021-9517/99 $30.00

abstraction of hydrogen atom from the methane molecule to form methyl radical can best be related to the basicity of the oxides, the more basic oxides being more active. Based on this finding, in the present work nitric oxide reduction by methane was investigated over pure CaO, which is one of the most basic oxides being used successfully for the OCM reaction. According to a recent review paper (29) concerning the current state of research on lean-NO_x catalysis, no reference is made to a published work for the HC-SCR of NO reaction over CaO surfaces. On the other hand, CO and H_2 have been studied as reducing agents of NO over the CaO surface (30–33).

In the present work, the catalytic behavior of CaO for the nitric oxide conversion by methane in the range 550–850°C was studied in the presence of excess oxygen in the range 1–10 mol%. The kinetic behavior of this reaction system was tested for NO feed concentrations in the range 500–6000 ppm and for CH_4 and O_2 feed concentrations in the range 0.5–4 mol%. The stability of the catalyst investigated and the effect of H_2O and CO_2 in the feed stream on NO reduction activity are also presented and discussed. Temperature-programmed desorption (TPD) experiments with NO have been conducted to study the interaction of adsorbed NO with the catalyst surface (i.e., bond strength, kinds of adsorbed NO), while the surface basicity of the CaO catalyst was studied by conducting TPD experiments of CO_2. The effects of gaseous oxygen and methane on the desorption properties of preadsorbed NO were investigated by conducting TPSR experiments with O_2/He, CH_4/He, and CH_4/O_2/He gas mixtures. In addition, the effects of preadsorbed CO_2 on the desorption kinetics of NO were studied by experiments on TPD of NO.

2. METHODS

The catalyst used in the present study was prepared by calcining CaO of high purity (99.95%, Alpha Products) for 24 h at 900°C. Due to this pretreatment of the catalyst, no further sintering was expected during reaction. The BET surface area after calcination was found to be less than 0.5 m^2/g.

The flow system used for conducting steady-state kinetic and catalyst evaluation measurements at atmospheric pressure consisted of a flow measuring and control system (MKS Instruments, Model 247C), mixing chambers, a quartz fixed-bed microreactor, an on-line gas chromatograph (GC) (Shimadzu 9A), and an on-line NO_x stack gas emissions analyzer (Teledyne Brown Engineering, Model 911/912). The flow system, the microreactor, and the analysis conditions pertaining to the gas chromatograph have been described in detail elsewhere (34).

The NO_x gas analyzer used the principle of chemiluminescence. The heart of the instrument was a photomultiplier tube assembly with a reaction chamber. Nitric oxide, both direct and converted from NO_2, was blended in the chamber with ozone produced by an ozone generator from oxygen. The intensity of the emitted light was in a linear relationship with the nitric oxide concentration. The photomultiplier tube enhanced and transduced the emitted light into a current. The latter then went to an electrometer and was displayed on the front panel of the analyzer. Separate readouts of NO alone and NO plus NO_2 combined were available.

The catalytic and kinetic experiments were performed using a feed mixture that consisted of NO in the range 500–6000 ppm, O_2 in the range 0–10 mol%, and CH_4 in the range 0.5–4 mol%, with He as the balance gas. Under these experimental conditions, reaction of NO with O_2 to form NO_2 in the gas lines (held at 120°C) outside the reactor was not observed. Before any data were taken, the catalyst sample was pretreated at 800°C in 20% O_2/He mixture at a flow rate of 50 ml/min for 1 h. The amount of catalyst sample used was varied in the range 50–300 mg and the reaction temperature in the range 500–850°C. The volume flow rate (F) of reactant gas mixture was kept constant at 50 ml/min (ambient), yielding a W/F ratio in the range $1–6 \times 10^{-3}$ g · min/ml. For the experiments to study the effects of H_2O in the feed stream on NO conversion, a feed gas mixture of about 5 mol% H_2O/He was prepared by flowing He through a deionized water saturator held at 33°C. The exit stream was then mixed with NO/He, CH_4/He, and O_2/He gas streams at the appropriate mass flow rates to produce the desired feed gas composition.

For kinetic measurements, the conversion of NO was always kept below 15%. Nitrogen reaction rates were then calculated from the product analyses using the differential reactor approximation, i.e., rate (mol g^{-1} min^{-1}) $= N_T \cdot y_i/W$, where N_T is the total molar flow rate (mol/min), y_i is the molar fraction of component i (i.e., N_2) expressed in ppm $\times 10^{-6}$, and W is the weight of the catalyst (g). For the present catalytic system, methane reacts with NO and O_2 according to the following competitive reaction scheme:

$$2NO + CH_4 + O_2 \rightarrow N_2 + CO_2 + 2H_2O, \quad [1]$$

$$CH_4 + 2O_2 \rightarrow CO_2 + 2H_2O. \quad [2]$$

The selectivity, α, for CH_4 reduction of NO to N_2, i.e., the ratio of the consumption rate of CH_4 for the NO reduction (reaction [1]) to the total consumption rate of CH_4 (reaction [1] + reaction [2]) is calculated based on

$$\alpha(\%) = \frac{0.5 \cdot y^{f}_{NO} \cdot X_{NO}}{y^{f}_{CH_4} \cdot X_{CH_4}} \times 100, \quad [3]$$

where y^{f}_{NO} and $y^{f}_{CH_4}$ are the inlet molar fractions of NO and CH_4, respectively, and X_{NO} and X_{CH_4} are the NO and CH_4 conversions, respectively. The value of 0.5 is the stoichiometric ratio of NO to CH_4 (reaction [1]). The fraction of CH_4 combusted by O_2 (reaction [2]) is given by $1 - \alpha$.

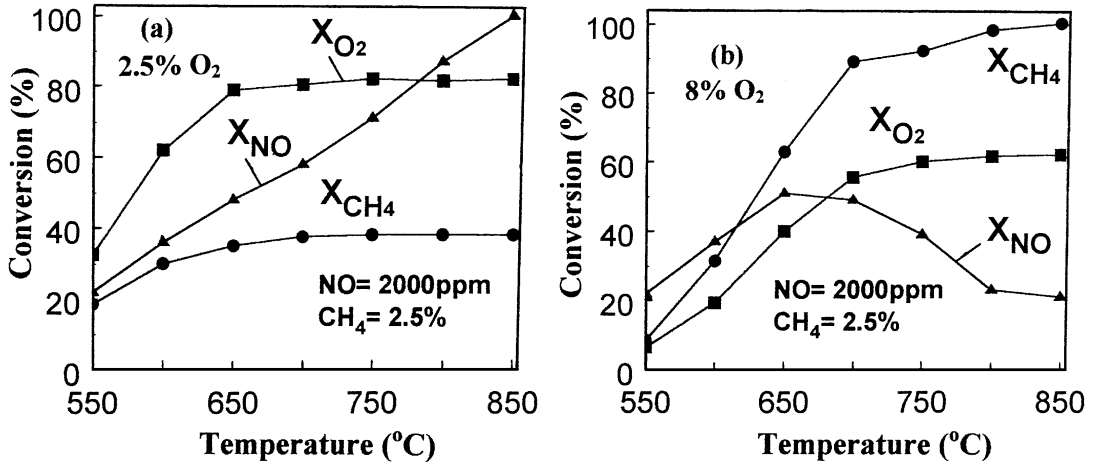

FIG. 1. (a) Conversions of NO, CH_4, and O_2 reactants as a function of temperature. Feed composition: NO = 2000 ppm, CH_4 = 2.5 mol%, O_2 = 2.5 mol%. (b) Conversions of NO, CH_4, and O_2 reactants as a function of temperature. Feed composition: NO = 2000 ppm, CH_4 = 2.5 mol%, O_2 = 8 mol%. $W/F = 6 \times 10^{-3}$ g/min/cm^3.

For the determination of reaction orders, a power rate law of the following form was used:

$$\text{rate} = k \cdot P_{CH_4}^{X} \cdot P_{NO}^{Y} \cdot P_{O_2}^{Z}. \quad [4]$$

The turnover frequencies (TOFs) of NO reduction by CH_4 were calculated after dividing the rate (μmol/g·s) by the irreversible NO uptake (μmol/g) at 50°C, the latter determined by TPD experiments.

TPD, temperature-programmed oxidation (TPO), and temperature-programmed surface reaction (TPSR) with CH_4 and CH_4/O_2/He of preadsorbed NO and various other transient experiments were conducted in a specially designed flow system which has been described elsewhere (35). Chemical analysis of gaseous streams during transients was done with an on-line mass spectrometer (VG Quadrupoles, SXP Elite) equipped with fast-response inlet capillary and data acquisition systems. The gaseous responses obtained by mass spectrometry were calibrated using standard mixtures. The gases during transient experiments were used at the flow rate of 40–50 ml/min (ambient). For TPD and TPSR measurements, the mass numbers (m/z) 15, 30, and 44 were used for CH_4, NO, and CO_2 (or N_2O), respectively. Very small amounts of N_2O but not of any NO_2 ($m/z = 46$) were detected during the TPSR experiments with O_2/He and CH_4/O_2/He mixtures.

3. RESULTS AND DISCUSSION

3.1. Catalyst Performance and Stability

NO reduction by CH_4 in the presence of oxygen was studied over CaO in the temperature range 550–850°C using 2000 ppm NO, 2.5 mol% CH_4, and two different O_2 concentrations (2.5 and 8.0 mol%) in the feed stream at a constant W/F ratio of 6×10^{-3} g·min/ml. This value corresponds to approximately 10000 h^{-1} (GHSV).

Figure 1a shows that for 2.5 mol% O_2 in the feed stream, NO conversion continuously increases with reaction temperature to reach the value of practically 100% at 850°C. At temperatures above 750°C, oxygen and methane conversions remain practically constant, obviously due to the remaining small concentrations of unreacted NO (reaction [1]). In this temperature region the conversion of CH_4 reaches the value of approximately 37%. Unlike zeolite-based catalysts, no bendover in activity is observed over the CaO catalyst under these experimental conditions (Fig. 1a).

The conversion-versus-temperature curves of Fig. 1b which correspond to 8 mol% O_2 in the feed stream are significantly different from those of Fig. 1a. In this case, NO conversion decreased significantly above 700°C. In the aforementioned experiments of Fig. 1, N_2, CO_2, and H_2O were the only reaction products observed. The N and C mass balances closed each within 2.5%. No higher hydrocarbons due to possible oxidative coupling of methane were detected in any circumstances, neither NO_2 nor N_2O.

Table 1 reports values of the selectivity parameter, α, as a function of reaction temperature for the experiments presented in Fig. 1. The highest selectivity value obtained is about 11%, and the lowest, 1%. These results obviously are not the desired ones since a large portion of CH_4 fed into the reactor is not used for the desired reduction of NO. On the other hand, it has to be stressed that for practical lean-deNO_x conditions the concentration of O_2 must be at least 5 mol%. Thus, to increase NO conversion for a constant value of GHSV, the concentration of the reducing agent (CH_4) must increase; the dependence of the rate of NO reduction on methane pressure is positive (see Section 3.2). The fact that 100% conversion of NO to N_2

TABLE 1

Selectivities for CH_4 Reduction of NO to N_2 According to the Results of Fig. 1 and Eq. [3]

	Selectivity, α (%)	
T (°C)	NO = 2000 ppm, CH_4 = 2.5%, O_2 = 2.5 mol%	NO = 2000 ppm, CH_4 = 2.5%, O_2 = 8 mol%
550	4.9	11.3
600	5.0	5.2
650	5.7	3.1
700	6.8	2.2
750	8.0	1.6
800	10.0	1.0
850	10.8	0.09

has been achieved under the conditions shown in Fig. 1a should be pointed out.

A comparison of the selectivity values reported by Vannice and co-workers (20) over La_2O_3- and Sm_2O_3-based catalysts should be made. In that work (20) the NO, CH_4, and O_2 feed concentrations used were 18000 ppm, 0.45 mol%, and 1 mol%, respectively. At 550°C the authors reported selectivity values in the range 35–65% over the above-mentioned metal oxide catalysts. However, Vannice and co-workers (20) used a y_{NO}/y_{CH_4} ratio of 4 in the feed stream, to be compared with the value of 0.08 used in the present work (50 times lower).

The effect of oxygen feed concentration on the catalyst activity of nitric oxide reduction with methane was determined by performing experiments at 650 and 770°C using 2000 ppm NO and 2.5 mol% CH_4, while the concentration of O_2 was varied between 0 and 10 mol%. In the absence of gaseous oxygen, methane and NO react over CaO according to the reaction

$$4NO + CH_4 \rightarrow 2N_2 + CO_2 + 2H_2O. \qquad [5]$$

Figure 2 shows that at 650°C the conversion of NO remained almost constant, even in the presence of excess O_2 in the feed stream of 10 mol%. On the other hand, at the higher temperature of 770°C the addition of oxygen up to concentrations of 10 mol% had a strong inhibiting effect. It must be noted that the stability of NO conversion versus O_2 feed concentration at 650°C shown in Fig. 2 is a very remarkable result. To our knowledge, it is the first time that behavior at 650°C (Fig. 2) is reported in the literature over metal oxide catalytic systems for the $CH_4/NO/O_2$ reaction. Vannice and co-workers studied the effect of oxygen (up to concentrations of 3 mol% O_2) on NO reduction with CH_4 over La_2O_3 catalyst (19). After using a GHSV = 12,400 h^{-1} (a value similar to that used in the present work), 1.4% NO and 0.35% CH_4 in the feed stream, at the reaction temperature of 650°C there was a maximum in the NO conversion (~10%) at about 0.5% O_2, while at 3% O_2 the conversion of NO reached 6%. However, in the present work with CaO at 650°C and using a GHSV = 10,000 h^{-1}, conversions as high as 50% were obtained up to 10% O_2 in the feed stream (Fig. 2).

The catalytic results shown in Figs. 1 and 2 are related to oxygen effects on important elementary steps of the reaction mechanism of the $CH_4/NO/O_2$ reaction over the CaO catalytic surface. Acke *et al.* (33) recently reported results from mechanistic studies of the NO + CO and NO + H_2 reactions over the CaO surface. The authors proposed that formation of N_2 from NO is based on the following steps: (i) an adsorbed $N_2O_2^-$ or $N_2O_2^{2-}$ species forms on a partially reduced CaO surface; (ii) the N–O bond in the aforementioned adsorbed dimers of NO breaks, leading to the formation of an N_2O intermediate product and to reoxidation of the CaO surface; (iii) at temperatures higher than 500°C, decomposition of N_2O to N_2 can be catalyzed by both the reduced and the unreduced CaO surfaces. In their study, Acke *et al.* (33) explained the role of reducing agents of CO and H_2 as being that of creating oxygen vacancies by an oxygen abstraction step via the formation of CO_2 and H_2O, respectively.

In the present case with CaO for the $NO/CH_4/O_2$ reaction, there is not yet conclusive experimental evidence for the mechanism of the reaction at hand. Recently, Vannice *et al.* (22) reported a kinetic and mechanistic study related to the $NO/CH_4/O_2$ reaction over La_2O_3-based catalysts. The authors proposed 13 elementary steps, where the rate-determining step was claimed to be the surface reaction of adsorbed CH_4 and NO_2 to form methyl species. Adsorbed NO_2 is formed by the surface reaction of adsorbed NO and O species, while adsorbed CO and OH species are also found as intermediates in the proposed mechanism. The adsorbed CO species is formed via the surface reaction of

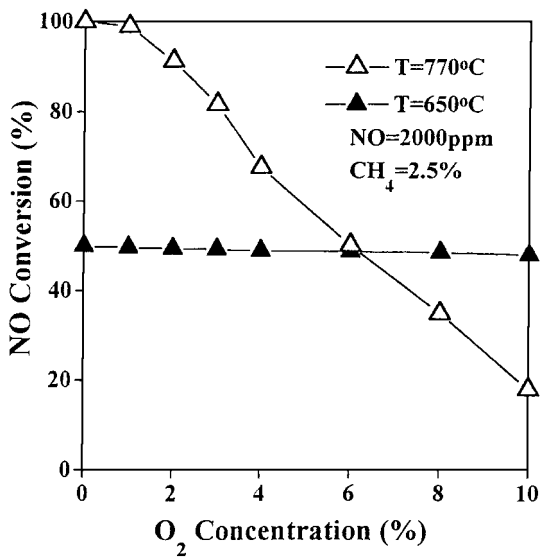

FIG. 2. Dependence of nitric oxide conversion on oxygen feed concentration at $T = 650$ and 770°C. Feed composition: NO = 2000 ppm, CH_4 = 2.5 mol%; $W/F = 6 \times 10^{-3}$ g/min/cm^3.

NCO and NO intermediate species. For the present CaO, OCM studies (36) have indicated that CO is produced together with the desired C_2-hydrocarbon products. As mentioned earlier, no detectable concentrations of these products were observed in the present catalytic reaction system. Explanations for the absence of C_2-hydrocarbons in the $NO/CH_4/O_2$ reaction over OCM metal oxide surfaces have been given elsewhere (19). In addition, it should be pointed out that adsorbed CO species might be formed directly from the reaction of CH_4/O_2 over the present CaO surface.

Based on the above-mentioned discussion, if the reoxidation step of the catalytic surface is an important step in the sequence of elementary steps of the reaction at hand, then this could explain the large decrease in NO conversion with increasing O_2 feed concentration observed at 770°C. Increasing the O_2 gas-phase concentration is expected to decrease the surface coverage of oxygen vacant sites and, therefore, the rate of $N_2O_2^-$ or $N_2O_2^{2-}$ species formation, the latter being likely important intermediate species for the formation of N_2. On the other hand, the results in Fig. 2 pertaining to $T = 650$°C cannot be explained based on the above-mentioned reasoning which might be used to explain the corresponding results obtained at $T = 770$°C. It seems that at the lower temperature of 650°C other additional elementary steps become more important than the surface reoxidation step. It is suggested that at 650°C the rate of reoxidation of the catalytic sites by gaseous oxygen is apparently very slow, while oxidation of these sites by NO or the intermediate NO_2 species is much faster. The large decrease in NO conversion with increasing O_2 feed concentration at 770°C must also be due to the CH_4 combustion reaction [2] mentioned before, the rate of the latter being much larger at 770°C than 650°C.

One of the major products of reactions [1] and [2] is carbon dioxide which is present in significant concentrations under integral reactor conditions. It is well known that calcium oxide reacts readily with CO_2 to form various kinds of surface carbonate species and bulk $CaCO_3$ as well (37). A study of the interaction of CO_2 with the catalyst surface and its effect on the conversion of NO is therefore of interest. The results reported in Fig. 3a reveal a decrease in NO conversion when 2.5 mol% CO_2 in the feed stream is used. The extent of reduction in NO conversion, however, varies with the reaction temperature. In the range 550–650°C, a larger inhibition of the NO reduction by CO_2 occurs as compared with that obtained in the range 700–850°C. From transient experiments to be presented (see Section 3.3), it is observed that NO adsorption takes place over the CaO surface in the temperature range 25–650°C. In addition, preadsorbed CO_2 at 100°C causes a significant decrease in NO chemisorption at 50°C. From these results it is suggested that the inhibiting effect of CO_2 under reaction conditions is due to competitive adsorption of CO_2 and NO on the same surface sites of CaO and/or to reduced adsorption of NO due to the formation of a stable calcium carbonate layer.

Investigations of the OCM reaction over La_2O_3/CaO catalysts have shown that CO_2, to a certain extent, prevents the adsorption of O_2 on the surface (38). Moreover, it was shown (39) that pretreatment of the catalyst with CO_2, which leads to the formation of surface carbonates, inhibits markedly the reversible activation of oxygen. These results indicate that activation of O_2 involves the same basic sites as activation of CO_2. Knowing that the role of dioxygen is to promote the activation of CH_4 via the formation of methyl radicals, the observed inhibition of NO conversion by CO_2 (Fig. 3a) could also be due to the reduced activation of methane.

Figure 3b presents results of the effects of 5 mol% H_2O in the feed stream containing 2000 ppm NO, 2.5 mol% CH_4,

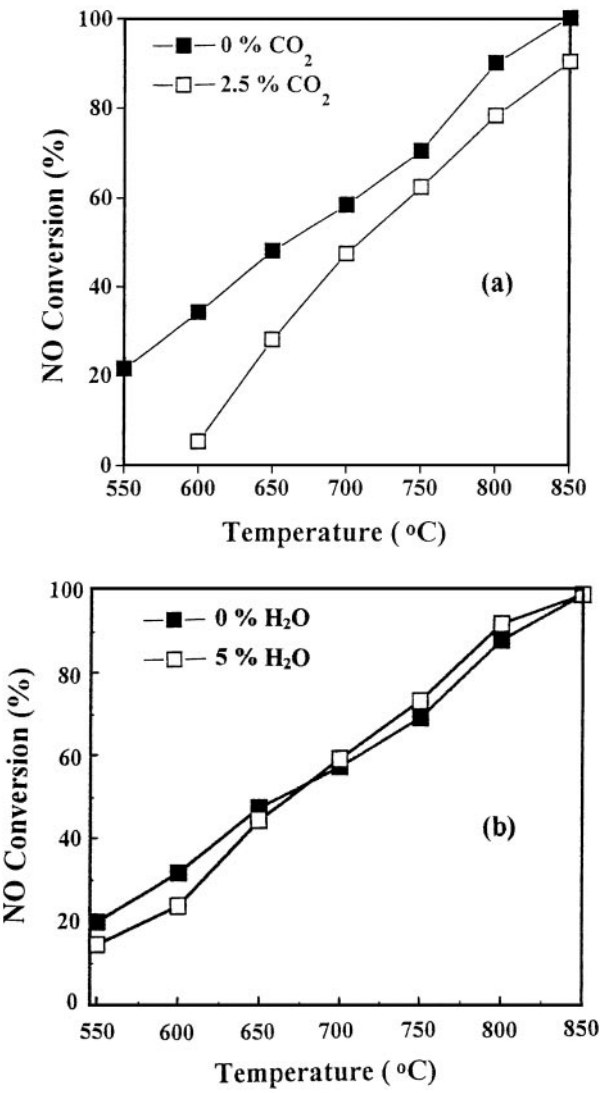

FIG. 3. (a) Effect of 2.5 mol% CO_2 in the feed stream on NO conversion as a function of reaction temperature. (b) Effect of 5 mol% H_2O in the feed stream on NO conversion as a function of reaction temperature. Feed composition: NO = 2000 ppm, CH_4 = 2.5 mol%, O_2 = 2.5 mol%; $W/F = 6 \times 10^{-3}$ g/min/cm^3.

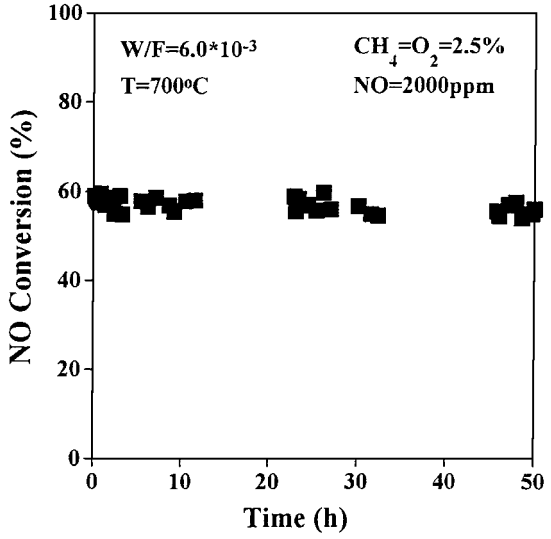

FIG. 4. Stability test over the CaO catalyst. Feed composition: NO = 2000 ppm, $CH_4 = 2.5$ mol%, $O_2 = 2.5$ mol%; $W/F = 6 \times 10^{-3}$ g/min/cm^3.

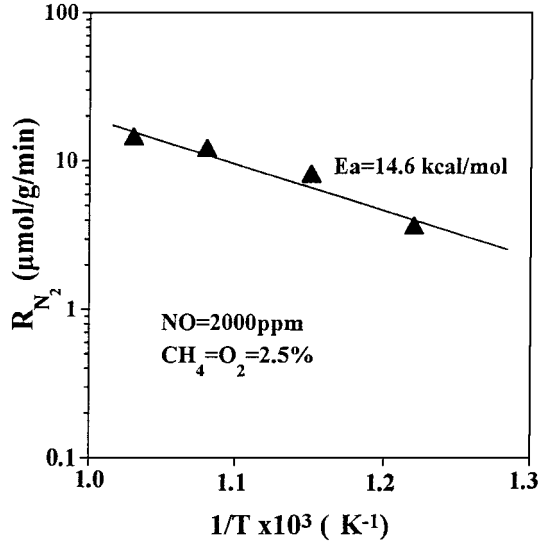

FIG. 5. Arrhenius plot of the rate of nitrogen production over the CaO catalyst. Feed composition: NO = 2000 ppm, $CH_4 = 2.5$ mol%, $O_2 = 2.5$ mol%.

and 2.5 mol% O_2 (balance He). A small inhibiting effect of H_2O on NO reduction is observed in the range 550–650°C, while a slight increase in NO conversion occurs in the range 700–850°C. The latter result is of practical importance. Based on the results in Fig. 3, CaO appears to have very good catalytic performance in the range 700–850°C under practical lean-deNO_x conditions when methane is used as a reducing agent.

The variation of NO conversion to N_2 as a function of time on stream at 700°C is illustrated in Fig. 4. In this experiment, the composition of the feed gas mixture was 2000 ppm NO, 2.5 mol% CH_4, and 2.5 mol% O_2. The initial conversion of NO was about 60% and decreased slightly with time on stream to approximately 55% after 50 h of continuous reaction. Thus, the CaO catalyst is observed to exhibit good stability with time-on-stream under the above-mentioned reaction conditions. It should also be emphasized that selectivity to N_2 remained at the 100% level during the entire course of the experiment.

3.2. Steady-State Kinetic Study

Figure 5 shows the Arrhenius plot of the rate of NO reduction to N_2 formation for NO feed concentration of 2000 ppm and for CH_4 and O_2 feed concentrations of 2.5 mol%. Results were obtained in the temperature range 550–700°C at NO conversions less than 15%. The apparent activation energy determined was found to be 14.6 kcal/mol (SD = 0.057).

In determining the reaction order with respect to nitric oxide, the partial pressures of CH_4 and O_2 were kept constant at 25 mbar (2.5 mol%), whereas the partial pressure of NO was varied between 1 and 6 mbar (1000 and 6000 ppm). Similarly, for determining the reaction order with respect to CH_4, the partial pressures of NO and O_2 were kept constant at 2 and 25 mbar, respectively, whereas the CH_4 partial pressure was varied between 5 and 40 mbar (0.5–4 mol%). A period of 30 min on stream was allowed at each temperature before any gas sample was taken for analysis.

Figures 6 and 7 present results of the rate of N_2 formation as a function of NO and CH_4 feed concentrations, respectively, at 650 and 770°C. Based on these results, the reaction orders with respect to NO and CH_4 (in the presence of 2.5 mol% O_2) were found to be 1.0 and 0.5, respectively,

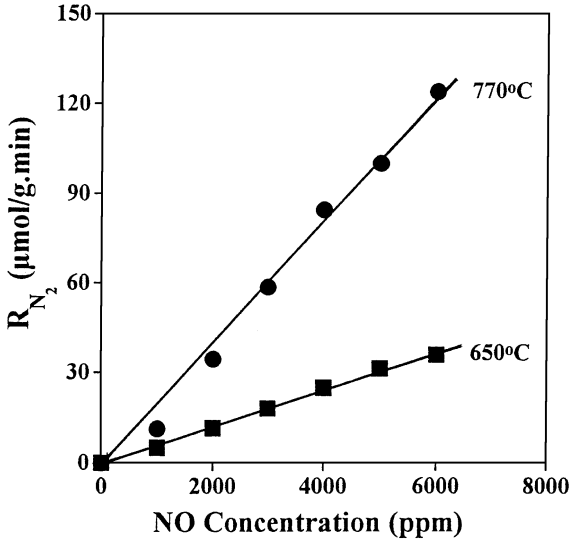

FIG. 6. Dependence of nitrogen production rate on nitric oxide feed concentration at $T = 650$ and 770°C. Feed composition: $CH_4 = 2.5$ mol%, $O_2 = 2.5$ mol%.

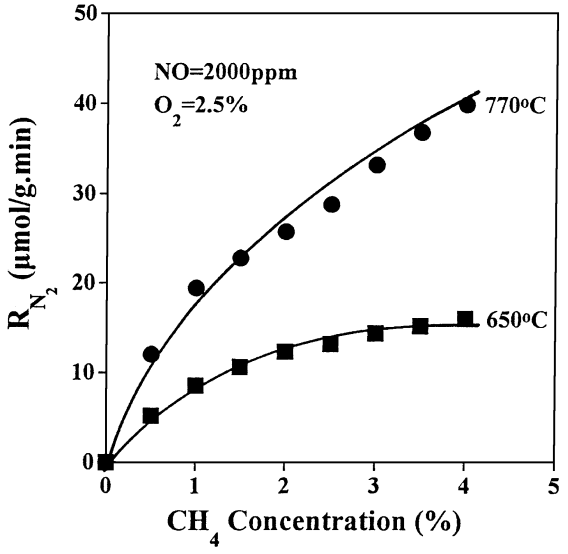

FIG. 7. Dependence of nitrogen production rate on methane feed concentration at $T = 650$ and 770°C. Feed composition: NO = 2000 ppm, $O_2 = 2.5$ mol%.

at both reaction temperatures. Under the feed conditions of 2.5 mol% CH_4, 2.5 mol% O_2, and 6000 ppm of NO, TOF values of 0.018 and 0.064 s^{-1} at 650 and 770°C, respectively, were calculated. A comparison is made between the TOF values reported by Vannice and co-workers (20) for Sr/La_2O_3 and Li/MgO catalysts and the values obtained for the present CaO under the reaction conditions of 1.8 mol% NO, 0.46 mol% CH_4, and 1 mol% O_2 in the feed stream at $T = 500$°C. After an extrapolation is made from the conditions used for CaO (NO = 0.6 mol%, $CH_4 = 2.5$ mol%, $O_2 = 2.5$ mol%, $T = 650$°C) to the conditions reported by Vannice and co-workers (20), a value of 1.65×10^{-3} s^{-1} is obtained for the CaO. This value is comparable to the value of 2.3×10^{-3} s^{-1} reported for Sr/La_2O_3 and much higher than the value of 0.32×10^{-3} s^{-1} reported for the Li/MgO catalyst (20).

The effect of O_2 concentration on the rate of NO reduction by CH_4 has also been determined at 650 and 770°C. In this case, 2 mbar NO and 25 mbar CH_4 were used in the feed stream, while the O_2 concentration was varied from 0 to 40 mbar (0–4 mol%). The corresponding experimental results obtained are presented in Fig. 8. It is evident that at 650°C the rate of N_2 formation increased with oxygen concentration up to 1 mol% and then practically remained constant up to oxygen concentrations of 4 mol%. The reaction order at O_2 concentrations below 1 mol% was found to be 0.25, while at higher concentrations it was found to be slightly negative. At the higher temperature of 770°C, the kinetic behavior was very similar to that observed at 650°C. The reaction order at O_2 concentrations below 1.5 mol% was found to be practically zero, while at higher concentrations it was found to be slightly negative. Behavior similar to that shown in Fig. 8 at 650°C has been reported by Vannice and co-workers (19) for the La_2O_3 catalyst. However, for the Li/MgO catalyst the presence of O_2 had a strong inhibiting effect (21).

The kinetic results presented in Fig. 8 could at first be considered as contradicting the catalytic results of Fig. 2. The relatively small decrease in the rate of N_2 formation with increasing O_2 feed concentration at 770°C is significantly different from the large decrease in NO conversion with increasing O_2 feed concentration (in the range 0–4 mol%). The reason is that under the integral reactor conditions of the experiments presented in Fig. 2 the rate of reaction varies significantly along the catalyst bed due largely to the variation in methane concentration (large methane conversions are achieved). On the other hand, in the case of the kinetic experiments (Fig. 8) the conversion of methane is kept small. The increase in reaction rate with increasing O_2 feed concentration in the range 0–1 mol% at 650°C (see Fig. 8) is compensated by the decrease in the rate along the catalyst bed due again to the large decrease in methane concentration for the integral reactor experiments shown in Fig. 2. Another reason for the additional decrease in the rate of NO consumption along the catalyst bed with increasing oxygen feed concentration is the effect of CO_2 (see Fig. 3a) which becomes larger in the case of the integral reactor experiments (large methane conversion and CO_2 formation due to reaction [2]).

The present kinetic results have provided information concerning the orders of reaction with respect to the three reactant species, namely, CH_4, O_2, and NO, and also the apparent activation energy of the reduction of NO with CH_4 in the presence of O_2. These results are compared and

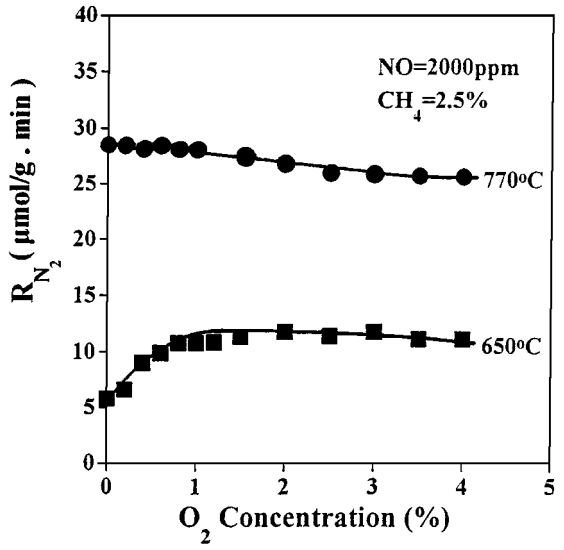

FIG. 8. Dependence of nitrogen production rate on oxygen feed concentration at $T = 650$ and 770°C. Feed composition: NO = 2000 ppm, $CH_4 = 2.5$ mol%.

discussed with respect to those obtained over similar catalytic surfaces, such as MgO, Li/MgO, La_2O_3, and Sr/La_2O_3 (21, 22). At 650°C, the reaction order with respect to CH_4 over the La_2O_3 and Sr/La_2O_3 catalysts was found to be 0.62 and 0.87, respectively (22), to be compared with the value of 0.5 determined in this work over the CaO surface. On the other hand, there is a large difference in the reaction order with respect to NO between the La_2O_3 and CaO surfaces. In the case of La_2O_3 (22), a reaction order of 0.53 was obtained, to be compared with the value of 1.0 obtained in the present work over CaO. This result may indicate that the nature of the chemisorption step of NO and of subsequent elementary steps that lead to N_2 formation is different over the two catalytic surfaces. It could also be true that the nature of the rate-determining step might be different over the two catalytic surfaces. A significant difference between the kinetic behavior of Li/MgO (21) and that of the present CaO catalyst appears in the reaction order with respect to O_2. In the case of Li/MgO catalysts, reaction orders between -0.43 and -0.73 have been reported, to be compared with the value of 0.25 obtained for the CaO surface. It is important to note that these reaction orders have been obtained after using similar O_2 feed concentrations. On the other hand, in the case of La_2O_3 and Sr/La_2O_3 catalysts (22) values similar to those for CaO were obtained, namely, 0.5 and 0.26, respectively.

As the feed oxygen concentration increases above 1 mol%, it was found in the present work that the reaction order with respect to O_2 becomes practically zero at 650°C and slightly negative at 770°C, results largely different from those observed at O_2 concentrations below 1 mol%. These results demonstrate that the partial pressure of gaseous oxygen controls important elementary steps that contain adsorbed oxygen species. It is noted that the nature of the rate-determining step may shift depending on the value of the partial pressure of oxygen. A mechanistic scheme based on a sequence of elementary steps has appeared in the literature for the present reaction system (22). It consists of 13 elementary steps where adsorbed atomic oxygen species participate in important steps from NO to form N_2, CO_2, and H_2O.

The apparent activation energy of the $CH_4/NO/O_2$ reaction over the present CaO catalyst was found to be about 15 kcal/mol, a value significantly lower than that obtained over La_2O_3 and Sr/La_2O_3 catalysts [26 kcal/mol (22)]. It should be pointed out that in the present case of CaO, the O_2 feed concentration used in the experiments for determining the apparent activation energy was 2.5 mol%, while in the case of La_2O_3-based catalysts it was 1 mol%. According to the previous discussion concerning the effects of O_2 partial pressure on the oxygen reaction order, and taking into account the large difference in the reaction order of NO exhibited by the CaO and La_2O_3-based catalysts, it seems reasonable that a significant change in the apparent activation energy of the overall reaction is observed for these catalytic materials.

3.3. *Transient Studies*

Various kinds of transient experiments were conducted to study qualitatively and quantitatively the chemical interaction of the NO molecule with the surface of CaO. Figure 9 shows the TPD and TPO response curves of desorbed NO under He and O_2/He flow, respectively. Following adsorption of NO from a 2 mol% NO/He mixture at 50°C for 15 min, the feed was changed to He for 5 min to purge the lines of the apparatus and to remove the gaseous NO from the microreactor. Then, the temperature was increased to 850°C at the rate of 20°C/min under He flow in the case of TPD, or under 1 mol% O_2/He flow in the case of TPO, while the nitric oxide (NO) and nitrous oxide (N_2O) desorbed from the catalyst surface were continuously monitored by mass spectrometry. Two distinct well-resolved desorption peaks were observed at 350 and 550°C in both cases, while the peak maximum intensity of the second peak is found to be lower than that of the first peak. In the case of TPD in He flow, a small broad peak in the range 50–250°C is observed (Fig. 9). In addition, some broadening of the second TPD peak at the higher temperatures is observed during the TPO experiment and a very small amount of N_2O is formed in the range 490–750°C (not shown in Fig. 9). The total amount of equivalent nitric oxide corresponding to the TPD response was found to be 32.3 μmol/g, and the amount corresponding to the TPO response was found to be practically the same (32.1 μmol/g). The amounts of NO desorbed

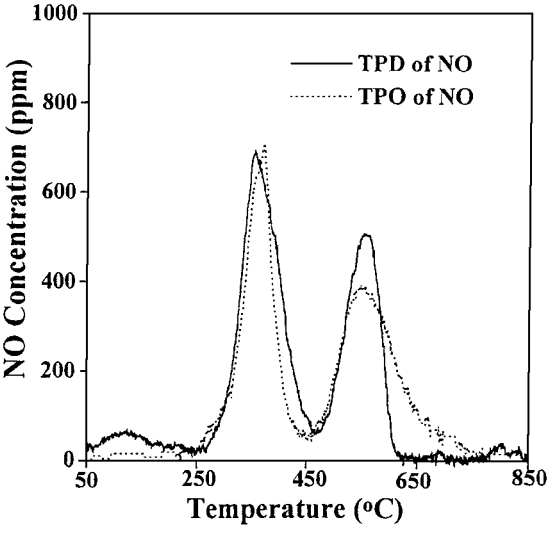

FIG. 9. Temperature-programmed desorption (TPD) and oxidation (TPO) of nitric oxide responses obtained according to the following gas delivery sequences: (a) 2 mol% NO/He (50°C, 15 min) → He (50°C, 10 min) → TPD ($\beta = 20$°C/min); (b) 2 mol% NO/He (50°C, 15 min) → He (50°C, 10 min) → TPO (1 mol% O_2/He, $\beta = 20$°C/min). Amount of catalyst used: 0.3 g; $Q = 40$ cm^3/min.

TABLE 2

Amount of Nitric Oxide Desorbed as Determined by Various Temperature-Programmed Transient Experiments

Experiment	Amount desorbed (μmol/g)	NO desorbed, first peak (%)
TPD	32.3	60
TPO	32.1	60
TPSR with CH_4/He	32.1	72
TPSR with CH_4/O_2	31.1	65

during the various temperature-programmed experiments are given in Table 2.

Figure 10 shows comparative results of TPD and TPSR experiments with CH_4. The latter experiment was performed by flowing a 1 mol% CH_4/He mixture over the catalyst on which NO had been adsorbed at 50°C. In the case of TPSR with CH_4, two well-resolved NO peaks are observed: the first one was centered at 350°C and the second one at 500°C. The amount of nitric oxide corresponding to the first peak is approximately twice the amount of the second peak. The total amount of desorbed NO is found to be 32.1 μmol/g. Very small amounts of CO_2 were measured in the range 550–850°C due to the reaction of CH_4 with the surface lattice oxygen of CaO. Although the amount of desorbed nitric oxide during the experiments presented in Fig. 10 is found to be the same (Table 2), qualitatively the results do exhibit certain differences. It is obvious that in the presence of CH_4 the desorption of NO observed at

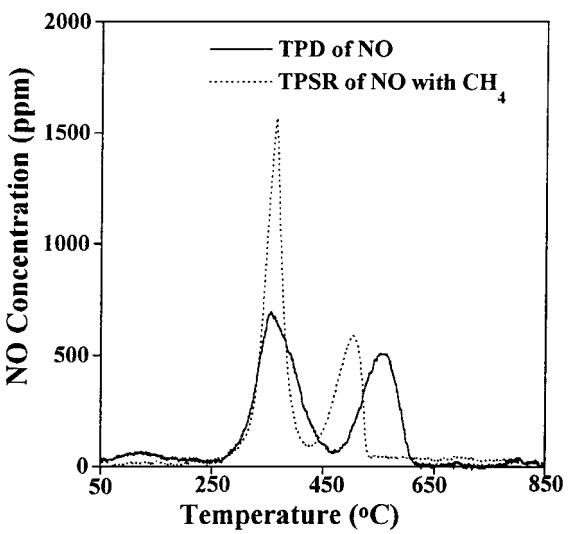

FIG. 10. Temperature-programmed desorption (TPD) and temperature-programmed surface reaction (TPSR) with CH_4 of nitric oxide responses obtained according to the following gas delivery sequences: (a) 2 mol% NO/He (50°C, 15 min) → He (50°C, 10 min) → TPD (β = 20°C/min); (b) 2 mol% NO/He (50°C, 15 min) → He (50°C, 10 min) → TPSR with CH_4 (1 mol% CH_4/He, $\beta = 20$°C/min). Amount of catalyst used: 0.3 g; $Q = 40$ cm^3/min.

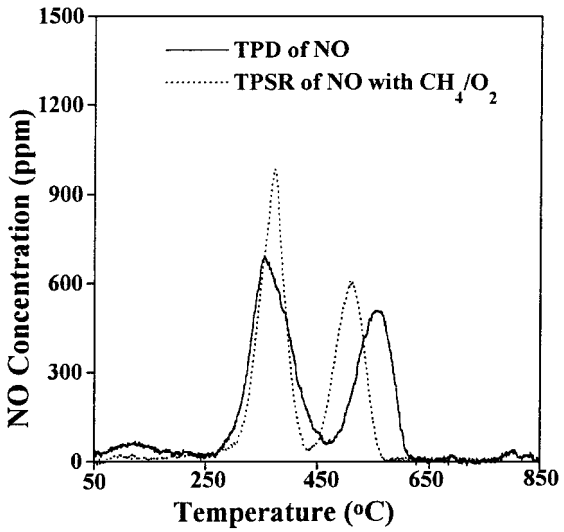

FIG. 11. Temperature-programmed desorption (TPD) and temperature-programmed surface reaction (TPSR) with CH_4/O_2/He of nitric oxide responses obtained according to the following gas delivery sequences: (a) 2 mol% NO/He (50°C, 15 min) → He (50°C, 10 min) → TPD (β = 20°C/min); (b) 2 mol% NO/He (50°C, 15 min) → He (50°C, 10 min) → TPSR with CH_4/O_2/He ($CH_4 = O_2 = 1$ mol%, $\beta = 20$°C/min). Amount of catalyst used: 0.3 g; $Q = 40$ cm^3/min.

higher temperatures in He flow is now shifted to lower temperatures, while the largest amount desorbed is observed in the lower temperature region of 250–400°C (Fig. 10).

Figure 11 shows comparative responses of TPD and TPSR experiments with CH_4/O_2/He ($CH_4 = O_2 = 1$ mol%) following NO chemisorption at 50°C for 15 min. In the case of TPSR with CH_4/O_2, two kinds of NO species are probed, based on the two resolved peaks observed at 350 and 500°C, as in the case of TPD and TPSR with methane. However, in the present case the ratio of the amount of NO desorbed corresponding to the two peaks is different. Very small amounts of N_2O but larger amounts of CO_2 were observed in the range 550–850°C (not shown in Fig. 11). The CO_2 formed is due to the combustion of CH_4. The quantitative results of desorbed NO for this TPSR experiment are presented in Table 2.

The results shown in Figs. 9–11 provide clear information concerning the influence of O_2 and CH_4 molecules on the chemisorbed state of NO over the CaO surface. The presence of gaseous O_2 leaves unaffected the kinetics of desorption of the first kind of chemisorbed NO, while it affects only slightly the kinetics of the high-temperature desorption of the second kind of chemisorbed NO. However, in the presence of gaseous CH_4, the kinetics of desorption of chemisorbed NO drastically changes; there exists a significant shift in the peak maximum temperature (T_M) of the high-temperature desorption peak and a large increase in the maximum desorption rate in the case of the low-temperature NO desorption peak. In the first case, there is a weakening of the chemisorption bond between the NO

molecule and the CaO surface induced by the presence of gaseous CH_4.

Detailed description of the modes of NO adsorption over metal oxide surfaces is still a controversial issue. This subject concerns the direction of electron transfer between the solid surface and the orbitals of the NO molecule (40–42), for example, whether an NO^- species is formed via an electron transfer from the metal oxide to the antibonding orbital of NO, thus weakening the N–O bond, or the opposite occurs by forming NO^+ species. In addition, it is not yet clear whether NO adsorption occurs with the N atom nearest the surface or with the O atom coordinated to anionic vacancies (41).

According to the recent work of Acke *et al*. (33), formation of NO dimers ($N_2O_2^-$ or $N_2O_2^{2-}$) over a CaO surface could occur, and these species have been considered as important intermediate species for the reduction of NO by CO or H_2 (33). Assuming that formation of NO dimers does occur over the present CaO surface, following NO chemisorption at low temperatures, then one possible explanation for the weakening of the NO adsorption bond is the existence of repulsions between adjacent adsorbed $H_3C^{\delta-}$–$H^{\delta+}$ and $N_2O_2^-$ or $N_2O_2^{2-}$ species. The former species are formed on adsorption of CH_4 onto Ca^{2+}–O^{2-} sites (28, 43), while the latter species are formed on adsorption of NO onto oxygen vacancy sites (33, 41). Another possible explanation for the weakening of the NO adsorption bond in the presence of methane might be the existence of an induced electron transfer within the chemisorbed state of NO by adsorbed CH_4 resulting in a reduced overlapping of the bonding orbitals of the molecular NO and the CaO surface. However, such a mechanism needs to be proved by providing experimental evidence.

The appearance of two well-resolved NO desorption peaks and a third small peak in the range 50–250°C strongly suggests the heterogeneity of the present CaO surface. Based on the discussion above, it is likely that molecularly adsorbed NO and $N_2O_2^-$ or $N_2O_2^{2-}$ species (nitric oxide dimer species) give rise to the appearance of the desorption peaks of NO shown in Figs. 9–11. Two nitric oxide desorption peaks have also been reported in the case of La_2O_3 (20).

The importance of surface basicity in the abstraction of hydrogen atoms from methane molecules to form methyl radicals has been pointed out by many investigators (28, 43). It has been proposed that an acid–base pair (M^{n+}_{LC} O^{2-}_{LC}) on the metal oxide surface is involved in the abstraction of the H atom from the methane molecule, according to the following scheme: When methane interacts with an acid–base pair having enough strength, it undergoes heterolytic C–H bond rupture, resulting in a CH_3^- ion attached on the acid site, while the H^+ ion interacts with the basic site. In the presence of O_2, an electron transfer from the carbanion CH_3^- to O_2 resulting in an O_2^- species is expected to take place, while the methyl radical can be released into the gas phase or be oxidized on the catalyst surface. In a recent kinetic study of the $NO/CH_4/O_2$ reaction over La_2O_3 and Sr/La_2O_3 catalysts (22), it was found that a rate-determining step involving the surface reaction of adsorbed CH_4 and NO_2 to generate methyl species was one of the restrictions of the kinetic model that best described the experimental results. The characterization of the surface basicity of CaO in terms of strength distribution and amount therefore becomes important.

The basicity of the surface of the present CaO catalyst was studied by TPD of preadsorbed CO_2 at 100°C, at a heating rate of 20°C/min and using helium as the carrier gas. Figure 12a shows the CO_2 TPD spectrum obtained. A

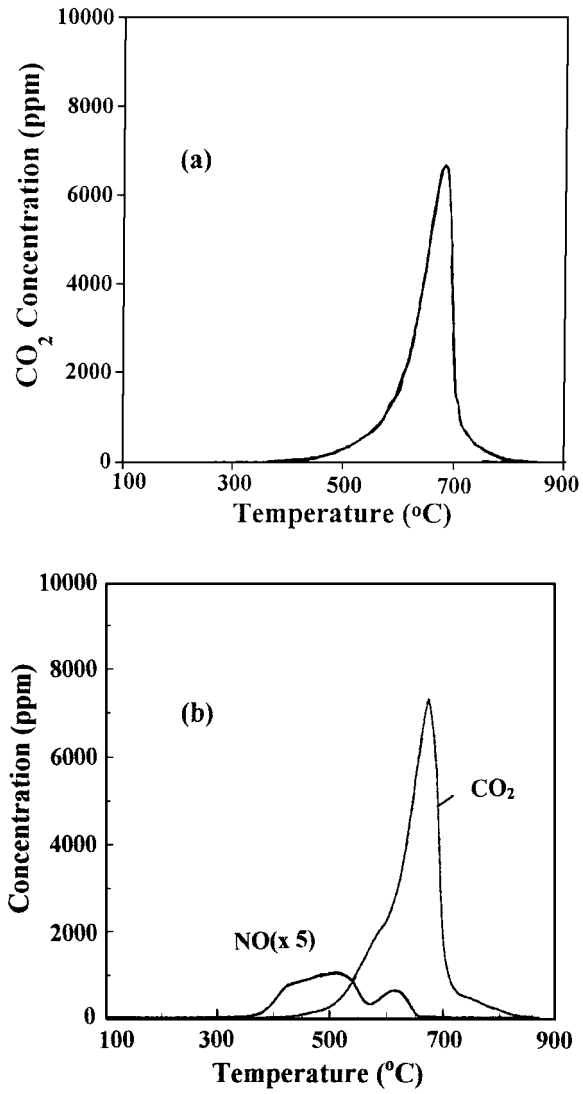

FIG. 12. (a) Temperature-programmed desorption (TPD) of CO_2 response obtained according to the gas delivery sequence 5 mol% CO_2/He (100°C, 15 min) → He (100°C, 15 min) → TPD ($\beta = 20$°C/min). (b) Temperature-programmed desorption of NO and CO_2 responses obtained according to the gas delivery sequence 5 mol% CO_2/He (100°C, 15 min) → He (100°C, 15 min) → cool down in He flow to 50°C → 2 mol% NO/He (50°C, 15 min) → He (50°C, 10 min) → TPD ($\beta = 20$°C/min). Amount of catalyst used: 0.3 g; $Q = 40$ cm^3/min.

single peak of desorbed CO_2 in the temperature range 400 to 800°C with peak maximum at $T_M = 680$°C and a small shoulder to the rising part of it appears. By integrating the TPD response curve, the amount of adsorbed CO_2 is found to be 155 μmol/g_{cat}. A comparison of this result with those obtained from similar basicity measurements over rare-earth metal oxides (43) leads to the conclusion that the present CaO sample has much higher surface basicity per gram of solid than the group of catalysts examined by Vannice *et al*. (22, 23) for NO reduction with CH_4. Catalytic activity tests over La_2O_3 performed under the same experimental reaction conditions as for CaO in this work (44) revealed that the CaO catalyst is more active than the La_2O_3 catalyst, especially at high temperatures. This may probably be related to the surface basicity differences exhibited by the two catalytic surfaces. In fact, La_2O_3 was found to have a significantly smaller amount of basic sites (17 μmol CO_2/g_{cat}) and also weaker basic sites (desorption of CO_2 in the range 250–650°C) than the CaO surface (44).

It is of interest to study the effect of preadsorbed CO_2 on NO chemisorption on the CaO surface since carbon dioxide is considered a major product of the present reaction and, also, it remains bound on the CaO surface even at 750°C (Fig. 12a). Figure 12b presents the desorption spectra of NO and CO_2 in a He TPD experiment according to the following experimental sequence. Carbon dioxide was adsorbed at 100°C for 15 min followed by a He purge to 100°C and subsequent cooling of the reactor to 50°C. The feed gas mixture was then changed to NO/He for 15 min followed by a switch to He for 10 min. The temperature of the catalyst sample was then increased to 900°C at the rate of 20°C/min in He flow.

Figure 12b shows clearly that a large decrease in the amount of desorbed NO takes place when compared with the result of Fig. 9 (6 μmol/g_{cat} vs 32.3 μmol/g_{cat}), while at the same time there occurs a change in the shape of the desorption spectrum of NO. On the other hand, the features of the desorption spectrum of CO_2 remain practically the same as those observed in the CO_2 TPD spectrum of Fig. 12a. The results in Figs. 9, 12a, and 12b strongly suggest that NO and CO_2 compete for the same adsorption sites, while the presence of adsorbed CO_2 influences the binding energy of adsorbed NO on the CaO surface. These results can provide some explanation of the inhibiting role of CO_2 in NO conversion under reaction conditions (Fig. 3a).

The present work also reports results of the transient hydrogenation and oxidation of carbon-containing species accumulated on the surface of CaO following reaction at 700°C with $CH_4/NO/O_2$/He mixture. Figure 13 presents results of a temperature-programmed hydrogenation (TPH) experiment with carbon species formed during reaction at 700°C for 1 h. Following reaction, the feed was changed to pure He at 700°C for 5 min followed by cooling of the reactor under He flow to 500°C. The feed was then changed to 1 mol% H_2/He and the temperature of the catalyst was

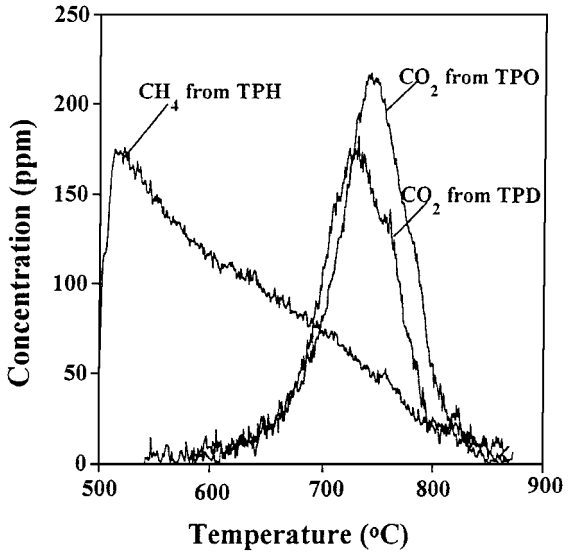

FIG. 13. Temperature-programmed hydrogenation (TPH), temperature-programmed oxidation (TPO), and temperature-programmed desorption (TPD) of adsorbed carbon-containing species formed during 1 h of $CH_4/NO/O_2$/He reaction at 700°C over the CaO catalyst. Gas delivery sequence: $CH_4/NO/O_2$/He (700°C, 1 h) → He (700°C, 5 min) → cool down in He flow to 500°C → 1% H_2/He (TPH) or 1% O_2/He (TPO) or He (TPD), $\beta = 30$°C/min. Amount of catalyst used: 0.3 g; $Q = 40$ cm^3/min.

increased at the rate of 30°C/min to 900°C to carry out a TPH experiment. A CH_4 peak is shown in Fig. 13 that is centered at about 520°C tailing out to 850°C. Integration of the CH_4 response resulted in an equivalent amount of carbon-containing species of 15 μmol/g_{cat}. Figure 13 also shows the CO_2 response obtained during a TPO experiment with carbon-containing species formed on exposure of the catalyst to the reaction mixture at 700°C for 1 h, as in the case of the TPH experiment. A rather symmetric peak is observed ($T_M = 750$°C) suggesting one kind of carbon species. In this TPO experiment, it was found that the amount of carbon removed as CO_2 is 9.7 μmol/g_{cat}. Note that significant quantities of CO_2 appeared at temperatures higher than 650°C during TPO, while a very small CH_4 response signal was observed above 650°C during TPH. Figure 13 also shows results of a TPD experiment in He flow of carbon-containing species formed during the reaction under conditions similar to those pertaining to the TPO experiment. The total amount of equivalent carbon corresponding to the CO_2 TPD response was found to be 8.2 μmol/g_{cat}, which is similar to the amount of CO_2 measured from the TPO response.

The position and shape of the CO_2 TPD and TPO responses shown in Figs. 12a and 13 probe for the presence of a carbonate-like species (i.e., ionic carbonate, unidentate or bidentate carbonate, bicarbonate) that might be formed on the CaO surface after reaction with the $NO/CH_4/O_2$/He mixture at 700°C for 1 h. If it is assumed that the only carbon-containing species formed on the catalyst surface

during reaction is that having a carbonate-like nature, then explanations must be provided for the different quantities of equivalent carbon measured by the TPH and TPD experiments of Fig. 13. It is speculated whether the larger quantity of equivalent carbon measured by TPH could be due to the presence of additional adsorbed carbon-containing species, such as CN–∗ and/or HCN–∗. The latter species may not be reactive toward either oxygen or surface reactions under He flow to give CO_2. The above-mentioned intermediate species have been proposed for the present reaction over La_2O_3-based catalysts (22). Despite the true chemical composition of the carbon-containing species formed under the present reaction conditions, it should be noted that a very small amount is accumulated on the CaO surface during 1 h of reaction at 700°C. This is believed to be the main reason for the very good stability of CaO under the reaction conditions investigated (Fig. 4).

4. CONCLUSIONS

The following conclusions can be derived from the results of the present work:

- CaO was found to be active for nitric oxide reduction by methane in the presence of oxygen and 100% selective toward N_2 formation in the temperature range 550–850°C.
- TOF values for the $NO/CH_4/O_2$ reaction over the present CaO catalyst compare favorably with the values reported in the literature over the best rare-earth metal oxide catalysts.
- The catalytic performance of CaO and the observed reaction rates of N_2 formation are considered much better than those reported in the literature for MgO and Li/MgO catalysts.
- The addition of oxygen at concentrations as high as 10 mol% has no effect on CaO catalyst activity at 650°C. However, at 770°C a significant decrease in NO conversion is evident.
- Carbon dioxide (2.5 mol% in the feed stream) is found to inhibit the reduction of nitric oxide, especially in the range 500–650°C. However, the inhibiting effect of 5 mol% H_2O in the feed stream is small in the range 500–650°C, while the influence of water on NO conversion in the range 700–850°C appears to be slightly positive.
- Temperature-programmed desorption studies of nitric oxide revealed two well-resolved desorption peaks, a result suggesting two kinds of adsorbed NO species on the CaO surface. The presence of 1 mol% O_2 has no effect on the desorption profile of NO, while the presence of 1 mol% CH_4 causes a shift of the high-temperature NO desorption to lower temperatures (decrease in the binding energy of NO with the CaO surface).
- Preadsorbed carbon dioxide is found to largely decrease the chemisorption of NO at 50°C and also to influence the kinetics of NO desorption during a TPD experiment.

ACKNOWLEDGMENTS

Financial support by the Commission of the European Community (Contract EV5V-CT92-0234) and the Research Committee of the University of Cyprus is gratefully acknowledged.

REFERENCES

1. Bosch, H., and Janssen, F. J. J. G., *Catal. Today* **2**, 369 (1988).
2. Beechman, J. W., and Hegedus, L. L., *Ind. Eng. Chem. Res.* **30**, 969 (1991).
3. Amiridis, M. D., Zhang, T., and Farrauto, R. J., *Appl. Catal. B* **10**, 203 (1996).
4. Hardee, J. R., and Hightower, J. W., *J. Catal.* **86**, 137 (1984).
5. Iwamoto, M., Yokoo, S., Sakai, K., and Kagawa, S., *J. Chem. Soc. Faraday Trans. 1* **77**, 1629 (1981).
6. Iwamoto, M., Yahiro, H., Shundo, S., Yu, Y., and Mizuno, N., *Appl. Catal.* **69**, L15 (1991).
7. Iwamoto, M., and Hamada, H., *Catal. Today* **10**, 57 (1991).
8. Sato, S., Hirabayashi, H., Yahiro, H., Mizuno, N., and Iwamoto, M., *Catal. Lett.* **12**, 193 (1992).
9. Li, Y., and Armor, J. N., *Appl. Catal. B* **1**, L31 (1992).
10. Li, Y., and Armor, J. N., *Appl. Catal. B* **2**, 239 (1993).
11. Witzel, F., Sill, G. A., and Hall, W. K., *J. Catal.* **149**, 229 (1994).
12. Hamada, H., Kintaichi, Y., Sasaki, M., Ito, T., and Tabata, M., *Appl. Catal.* **64**, L1 (1990).
13. Hamada, H., Kintaichi, Y., Sasaki, M., Ito, T., and Tabata, M., *Appl. Catal.* **70**, L15 (1991).
14. Sato, S. S., Hirabay, H., Yahiro, H., Mizuno, N., and Iwamoto, M., *Catal. Lett.* **12**, 193 (1992).
15. Inaba, M., Kintaichi, Y., and Hamada, H., *Catal. Lett.* **36**, 223 (1996).
16. Burch, R., Fornasiero, P., and Watling, T. C., *J. Catal.*, in press.
17. Harrison, B., Wyatt, M., and Gough, K. G., "Catalysis," Vol. 5, pp. 127–171. Roy. Soc. of Chemistry, London, 1982.
18. Maitra, A. M., Campbell, I., and Tyler, R. J., *Appl. Catal.* **85**, 27 (1992).
19. Zhang, X., Walters, A. B., and Vannice, M. A., *Appl. Catal. B* **4**, 237 (1994).
20. Zhang, X., Walters, A. B., and Vannice, M. A., *J. Catal.* **155**, 290 (1995).
21. Zhang, X., Walters, A. B., and Vannice, M. A., *J. Catal.* **146**, 568 (1994).
22. Vannice, M. A., Walters, A. B., and Zhang, X., *J. Catal.* **159**, 119 (1996).
23. (a) Zhang, X., Walters, A. B., and Vannice, M. A., *Appl. Catal. B* **7**, 321 (1996). (b) Shi, C., Walters, A. B., and Vannice, M. A., *Appl. Catal. B* **14**, 175 (1997).
24. Miller, J. A., and Bowman, C. T., *Prog. Energy Combust. Sci.* **15**, 287 (1989).
25. Yamada, F., Slafle, I. R., and Gutman, D., *Chem. Phys. Lett.* **83**, 409 (1981).
26. Davies, J. W., Grant, N. J. B., and Pilling, M. J., *J. Chem. Soc. Faraday Trans.* **87**, 2317 (1991).
27. Thorne, L. R., Branch, M. C., Chandler, D. W., Kee, R. J., and Miller, J. A., *in* "Proceedings, 21st Symposium (International) on Comb.," p. 965. The Comb. Inst., 1986.
28. Campbell, K. D., Zhang, H., and Lunsford, J. H., *J. Phys. Chem.* **92**, 750 (1988).
29. Fritz, A., and Pitchon, V., *Appl. Catal. B* **13**, 1 (1997).
30. Tsujimura, M., Furusawa, T., and Kunii, D., *J. Chem. Eng. Japan* **16**, 132 (1983).
31. Bertrand, R. R., Hoke, R. C., Shaw, H., and Skopp, A., *Am. Chem. Soc. Div. Fuel Chem.* **18**, 25 (1973).

32. Dam-Johansen, K., Hansen, P. F. B., and Rasmussen, S., *Appl. Catal. B* **5**, 283 (1995).
33. Acke, F., Panas, I., and Stromberg, D., *J. Phys. Chem. B* **102**, 5127 (1998).
34. Efstathiou, A. M., and Fliatoura, K., *Appl. Catal. B* **6**, 35 (1995).
35. Efstathiou, A. M., Papageorgiou, D., and Verykios, X. E., *J. Catal.* **141**, 612 (1993).
36. Efstathiou, A. M., and Verykios, X. E., *Appl. Catal. A* **151**, 109 (1997).
37. Philipp, R., and Fujimoto, K., *J. Phys. Chem.* **96**, 9035 (1992).
38. Yang, T., Feng, L., and Shen, S., *J. Catal.* **145**, 384 (1994).
39. Lacombe, S., Zanthoff, H., and Mirodatos, C., *J. Catal.* **155**, 106 (1995).
40. Iwamoto, M., *in* "Studies in Surface Science and Catalysis: Future Opportunities in Catalytic Separation Technology" (M. Misono, Y. Moro-oka, and S. Kuimura, Eds.), p. 121. Elsevier, Amsterdam, 1990.
41. Hightower, J. W., and van Leirsburg, D. A., *in* "The Catalytic Chemistry of Nitric Oxides" (R. L. Klimisch and J. G. Larson, Eds.). Plenum, New York, 1975.
42. Gandhi, H. S., and Shelef, M., *J. Catal.* **28**, 1 (1973).
43. Choudhary, V. R., and Rane, V. H., *J. Catal.* **130**, 411 (1991).
44. Fliatoura, K. D., and Verykios, X. E., in preparation.